Citation: Optics Express Vol. 21, Issue 23, pp. 27537-27549 (2013)
https://doi.org/10.1364/OE.21.027537

High reflectance ta-C coatings in the extreme ultraviolet

J. I. Larruquert,[1,*] L. V. Rodríguez-de Marcos,[1] J. A. Méndez,[1] P. J. Martin,[2] and A. Bendavid[2]

[1] *GOLD-Instituto de Óptica-Consejo Superior de Investigaciones Científicas, Serrano 144, 28006 Madrid, Spain*
[2] *CSIRO Materials Science and Engineering, PO Box 218 Lindfield, NSW 2070, Australia*
**larruquert@io.cfmac.csic.es*

Abstract: The extreme ultraviolet (EUV) reflectance of amorphous tetrahedrally coordinated carbon films (ta-C) prepared by filtered cathodic vacuum arc was measured in the 30-188-nm range at near normal incidence. The measured reflectance of films grown with average ion energies in the ~70-140-eV range was significantly larger than the reflectance of a C film grown with average ion energy of ~20 eV and of C films deposited by sputtering or evaporation. The difference is attributed to a large proportion of sp^3 atom bonding in the ta-C film. This high reflectance is obtained for films deposited onto room-temperature substrates. The reflectance of ta-C films is higher than the standard single-layer coating materials in the EUV spectral range below 130 nm. A self-consistent set of optical constants of ta-C films was obtained with the Kramers-Krönig analysis using ellipsometry measurements in the 190-950 nm range and the EUV reflectance measurements. These optical constants allowed calculating the EUV reflectance of ta-C films at grazing incidence for applications such as free electron laser mirrors.

OCIS codes: 120.4530 (Optical constants); 260.7200 (Ultraviolet, extreme); 310.6860 (Thin films, optical properties); 230.4040 (Mirrors); 140.2600 (Free-electron lasers, FELs); 350.6090 (Space optics).

References

1. R. C. Vehse, E. T. Arakawa, and J. L. Stanford, "Normal incidence reflectance of aluminum films in the wavelength region 800–2000 Å," J. Opt. Soc. Am. **57**, 551–552 (1967).
2. R. P. Madden, L. R. Canfield, and G. Hass, "On the vacuum ultraviolet reflectance of evaporated aluminium before and during oxidation," J. Opt. Soc. Am. **53**, 620–625 (1963).
3. W. J. Choyke, W. D. Partlow, E. P. Supertzi, F. J. Venskytis, and G. B. Brandt, "Silicon-carbide diffraction grating for the vacuum ultraviolet: feasibility," Appl. Opt. **16**, 2013–2014 (1977).
4. M. M. Kelly, J. B. West, and D. E. Lloyd, "Reflectance of silicon carbide in the vacuum ultraviolet," J. Phys. D **14**, 401–404 (1981).
5. J. I. Larruquert and R. A. M. Keski-Kuha, "Optical properties of hot-pressed B4C in the extreme ultraviolet," Appl. Opt. **39**, 1537-1540 (2000).
6. R. A. M. Keski-Kuha, J. F. Osantowski, H. Herzig, J. S. Gum, and A. R. Toft, "Normal incidence reflectance of ion beam deposited SiC films in the EUV," Appl. Opt. **27**, 2815–2816 (1988).
7. J. B. Kortright and D. L. Windt, "Amorphous silicon carbide coatings for extreme ultraviolet optics," Appl. Opt. **27**, 2841–2846 (1988).
8. G. M. Blumenstock and R. A. M. Keski-Kuha, "Ion-beam deposited boron carbide coatings for extreme ultraviolet," Appl. Opt. **33**, 5962–5963 (1994).
9. G. F. Jacobus, R. P. Madden, and L. R. Canfield, "Reflecting films of platinum for the vacuum ultraviolet," J. Opt. Soc. Am. **53**, 1084-1088 (1963).
10. W. R. Hunter, D. W. Angel, and G. Hass, "Optical properties of evaporated platinum films in the vacuum ultraviolet from 220 Å to 150 Å," J. Opt. Soc. Am. **69**, 1695-1699 (1979).
11. G. Hass, G. F. Jacobus, and W. R. Hunter, "Optical properties of evaporated iridium in the vacuum ultraviolet from 500 Å to 2000 Å," J. Opt. Soc. Am. **57**, 758-762 (1967).
12. J. T. Cox, G. Hass, J. B. Ramsey, and W. R. Hunter, "Reflectance and optical constants of evaporated osmium in the vacuum ultraviolet from 300 to 2000 Å," J. Opt. Soc. Am. **63**, 436-438 (1973).

13. Y. A. Uspenskii, V. E. Levashov, A. V. Vinogradov, A. I. Fedorenko, V. V. Kondratenko, Y. P. Pershin, E. N. Zubarev, and V. Y. Fedotov, "High-reflectivity multilayer mirrors for a vacuum-ultraviolet interval of 35-50nm," Opt. Lett. **23**, 771–773 (1998).
14. S. A. Yulin, F. Schaefers, T. Feigl, and N. Kaiser, "Enhanced reflectivity and stability of Sc/Si multilayers," Proc. SPIE **5193**, 155–163 (2004).
15. J. Gautier, F. Delmotte, F. Bridou, M. F. Ravet, F. Varniere, M. Roulliay, A. Jerome, and I. Vickridge, "Characterization and optimization of magnetron sputtered Sc/Si multilayers for extreme ultraviolet optics," Appl. Phys. A **88**, 719–725 (2007).
16. D. L. Windt, J. F. Seely, B. Kjornrattanawanich, and Y. A. Uspenskii, "Terbium-based extreme ultraviolet multilayers," Opt. Lett. **30**, 3186–3188 (2005).
17. B. Kjornrattanawanich, D. L. Windt, J. F. Seely, and Y. A. Uspenskii, "SiC/Tb and Si/Tb multilayer coatings for extreme ultraviolet solar imaging," Appl. Opt. **45**, 1765–1772 (2006).
18. B. Kjornrattanawanich, D. L. Windt, and J. F. Seely, "Normal-incidence silicon-gadolinium multilayers for imaging at 63 nm wavelength," Opt. Lett. **33**, 965–967 (2008).
19. M. Vidal-Dasilva, M. Fernández-Perea, J. A. Méndez, J. A. Aznárez, and J. I. Larruquert, "Narrowband multilayer coatings for the extreme ultraviolet range of 50-92 nm," Opt. Expr. **17**, 22773-22784 (2009).
20. J. I. Larruquert, M. Vidal-Dasilva, S. García-Cortés, L. Rodríguez-de Marcos, M. Fernández-Pereaa, J. A. Aznárez, and J. A. Méndez, "Multilayer coatings for the far and extreme ultraviolet," Proc. SPIE **8076**, 80760D (2011).
21. M. Fernández-Perea, R. Soufli, J. C. Robinson, Luis Rodríguez-De Marcos, J. A. Méndez, J. I. Larruquert, and E. M. Gullikson, "Triple-wavelength, narrowband Mg/SiC multilayers with corrosion barriers and high peak reflectance in the 25-80 nm wavelength region," Opt. Expr. **20**, 24018-24029 (2012).
22. H. R. Philipp, E. A. Taft, "Kramers-Kronig analysis of refiectance data for diamond," Phys. Rev. **136**, A1445-A1448 (1964)
23. R. A. Roberts, W. C. Walker, "Optical study of the electronic structure of diamond," Phys. Rev. **161**, 730-735 (1967).
24. K. Kurosawa, R. Sonouchi, A. Yokotani, W. Sasaki, M. Kattoh, Y. Takigawa, and K. Nishimura, "Fabrication, characteristics, and performance of diamond mirrors for vacuum ultraviolet excimer lasers," Opt. Eng. **34**, 1405-1409 (1995).
25. T. Sasano, E. Ishiguro, S. Mitani, and H. Tomimori, "Reflectivities of chemical vapor deposition diamond mirrors in the vacuum ultraviolet region," Rev. Sci. Instrum. **66**, 2211-2213 (1995).
26. P. W. May, "CVD diamond - a new technology for the future?," Endeavour Mag. **19**, 101-106 (1995).
27. D. L. Windt, W. C. Cash Jr., M. Scott, P. Arendt, B. Newnam, R. F. Fisher, A. B. Swartzlander, P. Z. Takacs, and J. M. Pinneo, "Optical constants for thin films of C, diamond, Al, Si, and CVD SIC from 24 A to 1216 A," Appl. Opt. **27**, 279–295 (1988).
28. S. Coraggia, F. Frassetto, J. A. Aznarez, J. I. Larruquert, J. A. Mendez, M. Negro, S. Stagira, C. Vozzi, and L. Poletto, "Carbon coatings for extreme-ultraviolet high-order laser harmonics," Nucl. Instr. Meth. A **635**, S43–S46 (2011).
29. J. I. Larruquert, R. A. M. Keski-Kuha, "Reflectance measurements and optical constants in the extreme ultraviolet of thin films of ion-beam-deposited carbon," Opt. Comm. **183**, 437–443 (2000).
30. P. J. Martin, A. Bendavid, "Review of the filtered vacuum arc process and materials deposition," Thin Solid Films **394**, 1-15 (2001).
31. A. C. Ferrari, A. Libassi, B. K. Tanner, V. Stolojan, J. Yuan, L. M. Brown, S. E. Rodil, B. Kleinsorge, and J. Robertson, "Density, sp^3 fraction, and cross-sectional structure of amorphous carbon films determined by x-ray reflectivity and electron energy-loss spectroscopy," Phys. Rev. B **62**, 11089-11103 (2000).
32. F. Xiong, Y. Y. Wang, and R. P. H. Chang, "Complex dielectric function of amorphous diamond films deposited by pulsed-excimer-laser ablation of graphite," Phys. Rev. B **48**, 8016-8023 (1993).
33. S. Waidmann, M. Knupfer, J. Fink, B. Kleinsorge, and J. Robertson, "Electronic structure studies of undoped and nitrogen-doped tetrahedral amorphous carbon using high-resolution electron energy-loss spectroscopy," J. Appl. Phys. **89**, 3783-3792 (2001).
34. P. J. Martin, A. Bendavid, T. J. Kinder, and L. Wielunski, "The deposition of TiN thin films by nitrogen ion assisted deposition of Ti from a filtered cathodic arc source," Surf. Coat. Technol., **86-87**, 271-278 (1996).
35. Shi Xu , D. Flynn , B. K. Tay , S. Prawer , K. W. Nugent , S. R. P. Silva , Y. Lifshitz, and W. I. Milne, "Mechanical properties and Raman spectra of tetrahedral amorphous carbon films with high sp^3 fraction deposited using a filtered cathodic arc," Phil. Mag. B **76**, 351-361 (1997).
36. M. C. Polo, J. L. Andújar, A. Hart, J. Robertson, and W. I. Milne, "Preparation of tetrahedral amorphous carbon films by filtered cathodic vacuum arc deposition," Diam. Rel. Mater. **9**, 663–667 (2000).
37. B. K. Tay, X. Shi, L. K. Cheah, and D. I. Flynn, "Optical properties of tetrahedral amorphous carbon films determined by spectroscopic ellipsometry," Thin Solid Films **308–309**, 268–272, (1997).
38. R. Klucker, M. Skibowski, and W. Steinmann, "Anisotropy in the optical transitions from the π and σ valence bands of graphite," Phys. Stat. Sol. B **65**, 703–710 (1974).
39. R. A. M. Keski-Kuha, J. F. Osantowski, and H. Herzig, J. S. Gum, and A. R. Toft, "Normal incidence reflectance of ion beam deposited SiC films in the EUV," Appl. Opt. **27**, 2815-2816 (1988).
40. G. M. Blumenstock, R. A. M. Keski-Kuha, and M. L. Ginter, "Extreme ultraviolet optical properties of ion-beam-deposited boron carbide thin films," Proc. SPIE **2515**, 558–564 (1995).

41. G. Hass, G. F. Jacobus, and W. R. Hunter, "Optical Properties of Evaporated Iridium in the Vacuum Ultraviolet from 500 Å to 2000 Å," J. Opt. Soc. Am. **57**, 758-760 (1967).
42. J. T. Cox, G. Hass, J. B. Ramsey, and W. R. Hunter, "Reflectance and optical constants of evaporated osmium in the vacuum ultraviolet from 300 to 2000 Å," J. Opt. Soc. Am. **63**, 435–438 (1973).
43. M. Chhowalla, J. Robertson, C. W. Chen, S. R. P. Silva, C. A. Davis, G. A. J. Amaratunga, and W. I. Milne, "Influence of ion energy and substrate temperature on the optical and electronic properties of tetrahedral amorphous carbon (ta-C) films," J. Appl. Phys. **81**, 139-145 (1997).
44. A. LiBassi, A. C. Ferrari, V. Stolojan, B. K. Tanner, J. Robertson, and L. M. Brown, "Density, sp^3 content and internal layering of DLC films by X-ray reflectivity and electron energy loss spectroscopy," Diam. Rel. Mater. **9**, 771–776 (2000).
45. Z. Y. Chen, J. P. Zhao, "Optical constants of tetrahedral amorphous carbon films in the infrared region and at a wavelength of 633 nm," J. Appl. Phys. **87**, 4268-4273 (2000).
46. P. J. Fallon, V. S. Veerasamy, C. A. Davis, J. Robertson, G. A. J. Amaratunga, W. I. Milne, and J. Koskinen, "Properties of filtered-ion-beam-deposited diamondlike carbon as a function of ion energy," Phys. Rev. B **48**, 4777 (1993).
47. B. K. Tay, X. Shi, L. K. Cheah, and D. I. Flynn, "Growth conditions and properties of tetrahedral amorphous carbon films," Thin Solid Films **308–309**, 199–203 (1997).
48. T. A. Friedmann, J. P. Sullivan, J. A. Knapp, D. R. Tallant, D. M. Follstaedt, D. L. Medlin, and P. B. Mirkarimi, "Thick stress-free amorphous-tetrahedral carbon films with hardness near that of diamond," Appl. Phys. Lett. **71**, 3820-3822 (1997).
49. A. A. Balandin, M. Shamsa, W. L. Liu, C. Casiraghi, and A. C. Ferrari, "Thermal conductivity of ultrathin tetrahedral amorphous carbon films," Appl. Phys. Lett. **93**, 043115 (2008).
50. G. Reiße, S. Weißmantel, "Excimer-Laser Assisted Deposition of Carbon and Boron Nitride-Based High-Temperature Superconducting Films," in *Excimer Laser Technology, Part II*, D. Basting, G. Marowsky, eds., chapter 17, p. 335-350, Springer Berlin Heidelberg, 2005.
51. R. Delmdahl, S. Weissmantel, and G. Reisse, "Diamondlike carbon films," Adv. Mater. Process. **168**, 23-25 (2010).
52. M. Chhowalla, Y. Yin, G. A. J. Amaratunga, D. R. McKenzie, and T. Frauenheim, "Highly tetrahedral amorphous carbon films with low stress," Appl. Phys. Lett. **69**, 2344-2346 (1996).
53. J. Robertson, "Diamond-like amorphous carbon," Mater. Sci Engin. R **37**, 129-281 (2002).
54. B. L. Henke, E. M. Gullikson, and J. C. Davis, "X-ray interactions: photoabsorption, scattering, transmission, and reflection at E=50–30000 eV, Z=1–92," At. Data Nucl. Data Tables **54**, 181–342 (1993).
55. http://henke.lbl.gov/optical_constants/.
56. M. Tan, J. Zhu, A. Liu, Z. Jia, and J. Han, "Effects of mass density on the microhardness and modulus of tetrahedral amorphous carbon films," Mater. Lett. **61**, 4647–4650 (2007).
57. Downloaded from the following web of Physical Reference Data, Physics Laboratory at NIST: http://physics.nist.gov/PhysRefData/FFast/Text/cover.html.
58. M. Altarelli and D. Y. Smith, "Superconvergence and surn rules for the optical constants: physical meaning, comparison with experiment, and generalization," Phys. Rev. B **9**, 1290-1298 (1974).
59. E. Shiles, T. Sasaki, M. Inokuti, and D. Y. Smith, "Self-consistency and sum-rule tests in the Kramers-Kronig analysis of optical data: applications to aluminum," Phys. Rev. B **22**, 1612 (1980).
60. B. Steeg, L. Juha, J. Feldhaus, S. Jacobi, R. Sobierajski, C. Michaelsen, A. Andrejczuk, and J. Krzywinski, "Total reflection amorphous carbon mirrors for vacuum ultraviolet free electron lasers," Appl. Phys. Lett. **84**, 657-659 (2004).

1. Introduction

Many applications demand efficient mirrors for the extreme ultraviolet (EUV; here it refers to wavelengths in the 10-100-nm range; the 100-200-nm range will be referred to as the far ultraviolet, FUV). Thus, imaging targets in the solar system and universe at fundamental spectral lines in the EUV is often challenging due to the low intensity of the sources and to the modest reflectance of the coatings. EUV mirrors with high reflectance are also required for other applications such as synchrotron radiation, free electron lasers (FEL), spectroscopy, and plasma diagnostics. The lack of transparent materials at wavelengths above ~50 nm requires the use of mirrors with a single-layer coating and hence with a relatively low reflectance. Aluminum is an exception to this rule, with a high reflectance down to its plasma wavelength at 83 nm [1]; however, Al slightly oxidizes in contact with the atmosphere, which destroys its EUV reflectance and which is unavoidable since no protective coating is available that is transparent below ~105 nm, the cutoff of LiF [2]. In the EUV range, chemical-vapor-deposited (CVD) SiC coatings [3,4] and hot-pressed B_4C [5] are among the few stable materials that provide the largest known reflectance below ~100 nm down to ~60 nm, which is

in the range of ~30-50%. However, CVD SiC films must be deposited onto substrates at very high temperatures, whereas hot-pressed B_4C is a bulk material that is prepared at an extremely high temperature. In many practical applications, the mirror substrate must be kept close to room temperature during coating deposition. With this limitation, sputter-deposited coatings of SiC [6,7], along with B_4C [8], provide a reflectance of ~30-35% in the 60-100-nm range after the material has been exposed to the atmosphere for extensive periods. Below 65 nm, single layers of a few metals like Pt [9,10], Ir [11], and Os [12], have a relatively high reflectance of up to ~20-35% in the ~45-70 nm range. In spite of the lack of transparent materials, moderately high reflectance, narrowband multilayer coatings based on the transparency of Sc [13,14,15], Tb [16,17], Gd [18], Yb [19], Eu [20], and Mg [21] films have been developed recently.

Bulk carbon in the diamond allotrope was found to have a record reflectance in the EUV at wavelengths shorter than ~110 nm down to ~50 nm [22,23]. However, bulk diamond mirrors are impractical in real applications. CVD diamond films have also been developed with a reflectance close to natural diamond [24,25], and this material is more suitable in practice. The preparation of CVD diamond films involves large substrate temperatures, in the range of ~1000-1400 K [26]; Kurosawa et al. [24] mention a temperature between 1050 and 1270 K to grow crystalline diamond particles and an unspecified temperature below 970 K to grow amorphous particles. Heating the mirror substrate at such high temperatures may not be either possible or desirable in most cases.

Carbon films can also be deposited onto room-temperature substrates either by evaporation [27,28] or sputtering techniques [29]; unfortunately, their reflectance is substantially smaller than that of bulk or CVD diamond. Ion-beam-sputter deposited (IBD) C films have a higher EUV reflectance than films deposited by evaporation, which has been attributed to the larger average energy of condensing C atoms in IBD compared to evaporation [29]; for IBD C films, a slight increase in the average energy of condensing atoms was seen to result in an increase in the EUV reflectance of the resulting films and this was attributed to a larger content of sp^3 bonding, the bonding of C in diamond [29]. This behaviour suggested that C films grown with impinging C atoms with optimum energy for the highest proportion of sp^3 bonding might result in a higher EUV reflectance [29].

C films with largest sp^3 bonding can be prepared by filtered cathodic vacuum arc (FCVA), among other techniques. The technique involves the arc evaporation of carbon and the creation of ~70% singly charged carbon ions with an energy of approximately 20-25 eV [30]. The positively charged ions can subsequently be accelerated to higher energies by the application of a negative substrate bias. The ions condense onto a room temperature substrate forming amorphous tetrahedrally coordinated carbon films (ta-C) with a high sp^3 content, the magnitude of which can be optimised by the level of the applied substrate bias. The deposited films have a density not far from bulk diamond. C films with an enhanced proportion of sp^3 bonding versus sp^2 (graphitic) bonding are called Diamond-Like Carbon (DLC); the term ta-C is used for DLC films when the proportion of sp^3 bonding is the largest, which is in the range of ~85% [31].

Other than EUV reflectance, ta-C films have remarkable properties, such as mechanical hardness, chemical inertness, ultrasmoothness, and thermal stability, which are comparable with those of natural diamond. These are valuable properties for a mirror coating that may have to work in adverse conditions, such as in space or in a FEL.

Little information is available on the optical properties of ta-C films in the EUV. The EUV dielectric constant of ta-C films was determined from electron energy-loss spectroscopy [32,33], but to the best of our knowledge, no optical measurements, particularly reflectance, have been performed on ta-C films in the EUV. This paper reports on the EUV reflectance of

ta-C films deposited by FCVA. Section 2 gives a brief description of the experimental techniques used for thin film preparation and optical characterization. In Section 3 we present the EUV reflectance of ta-C films prepared by FCVA with various average energies of the condensing C ions, along with the optical constants of the films in the 190-950 nm range, which were determined using ellipsometry. Finally, Kramers-Krönig analysis with reflectance data extended to a wide spectral range was used to obtain the optical constants of ta-C films in the EUV.

2. Experimental techniques

The films were deposited using a filtered cathodic arc system described previously [34]. A general description of the technique can be found in Martin et al. [30]. The arc source was operated at 60 A dc and used a pure carbon cathode (99.999% Plasma Materials), 60 mm in diameter. The substrates were mounted at the exit of the filtered arc source and were semiconductor grade polished silicon wafers (<100>) with a resistivity of 0.6-1.2 Ωcm. During deposition, the substrates were at ambient temperature and the area of deposition was approximately 50 mm^2. The positive ion current at the substrate was measured with a biased shutter. The current was typically 100 mA over an area of the substrate. The film thickness was controlled by the deposition time and the typical deposition rate was 30-40 nm/min. The temperature of the substrate was measured by a thermocouple and did not exceed 40°C during deposition. The energy of the C ions impinging on the growing film could be tuned by adjusting the level of the negative bias voltage applied to the substrate in the 0-120-V range, which, for singly charged ions, the bias voltage added an energy to the ions ranging from 0 to 120 eV. The total energy of the ions impinging on the substrate is the energy of the ions as created in the arc, which is ~20 eV, plus the energy given by the bias voltage.

EUV reflectance was measured with GOLD's reflectometer. It has a grazing-incidence, toroidal-grating monochromator, in which the entrance and exit arms are 146º apart. The monochromator covers the 12.5-200-nm spectral range with two Pt-coated diffraction gratings that operate in the long (250 l/mm) or in the short (950 l/mm) spectral sub-ranges. The reflectometer operates with spectral lines that are generated in a windowless discharge lamp. The lamp is fed with various pure gases or gas mixtures with which the lamp can generate many spectral lines to cover the spectral range of interest. The beam divergence was ~5 mrad. The sample holder can fit samples up to 50.8x50.8 mm^2. A channel electron multiplier with a CsI-coated photocathode was used as the detector. Reflectance was obtained by alternately measuring the incident intensity and the intensity reflected by the sample. Reflectance measurements were performed at 5º from the normal. Reflectance uncertainty is estimated to be within ±2%.

Ellipsometry measurements were performed with a SOPRALAB GES5E spectroscopic ellipsometer. The incidence angle at which measurements were performed, 68° from the normal, was optimized by confining the spectral distribution of cosΔ symmetrically around zero in order to maximize accuracy. Ellipsometry measurements were performed to obtain thin film optical constants; ellipsometry is a precise technique and it is highly adequate when Si wafers are used as substrates.

3. Results and discussion

A. EUV reflectance

Five carbon samples were prepared in this research with the following bias voltage values: 0, 50, 80, 100, and 120 V, which are named as samples 1 to 5. The estimated average energy of the impinging ions on the growing film is ~20, 70, 100, 120, and 140 eV. Table 1 summarizes bias voltage, approximate average ion energy, and film thickness. Figure 1 displays the EUV-FUV reflectance of the five C samples as a function of wavelength. Two features are remarkable in the figure. One is that there is no significant reflectance difference over the

samples grown with approximate average ion energies in the 70 to 140 eV range, and the differences over the samples are within the measurement uncertainty. This is attributed to the highest sp^3 bonding that has been reported for films deposited with C ion energies in the ~50-150 eV range [35,36]. The other feature is that the films grown with ~70 eV or higher average energy have a substantially higher reflectance in the whole spectral range than the film grown with 0-V bias voltage, hence ~20-eV ion energy. This higher reflectance is coherent with the aforementioned highest sp^3 bonding for films grown in this range of C ion energies, along with the large EUV reflectance of bulk diamond, with 100% sp^3 bonding. The four samples grown with ion energy of ~70 eV and above (samples 2 to 5) correspond then to ta-C films. However, sample 1 estimated ion energy is insufficient to result in a ta-C film. The effect of different film thicknesses over the samples is mostly negligible due to the short attenuation length of the material and to the relatively thick films involved; hence all samples can be considered opaque in most of the measured range. In order to estimate the effect of thickness, reflectance was calculated using the optical constants obtained in sub-section 3.B; the reflectance difference calculated for the film thicknesses of samples 2 to 5 was limited to 0.04% (relative) in the range of largest reflectance (55-150 nm). The largest reflectance dependence on thickness is obtained at the longest wavelengths, as can be seen in Fig. 1, due to the smaller *k* of ta-C films, which will be displayed in the next sub-section. The large reflectance difference observed for samples grown with 50-V voltage or larger with respect to the sample grown with 0-V voltage cannot be explained in terms of thickness either: such a film thickness difference is only responsible of a 0.7% calculated reflectance difference (relative) in the range of largest reflectance (55-150 nm).

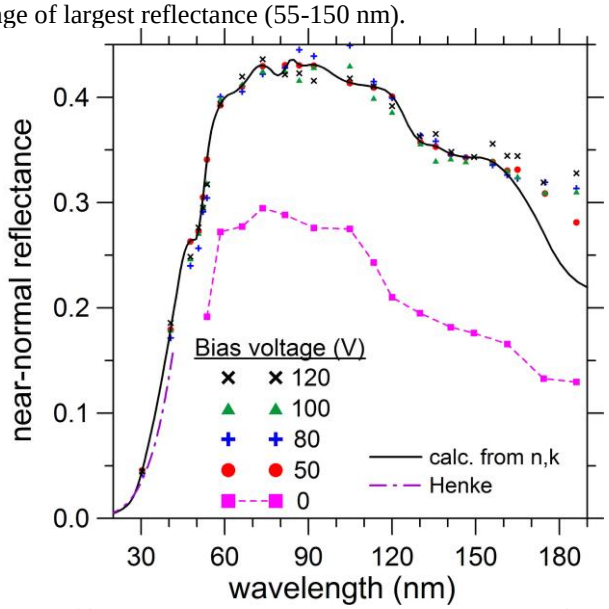

Fig. 1. EUV-FUV reflectance of five C samples grown with the plotted bias voltage as a function of wavelength. The estimated average C ion energy is given in Table 1. Solid line: reflectance calculated with the present optical constants. The semi-empirical data of Henke et al. [54] are also shown.

Table 1. Bias voltage, C-ion energy, and film thickness of the prepared samples

Sample	Bias voltage (V)	Approx. average C ion energy (eV)	Thickness (nm)
1	0	20	47.0
2	50	70	71.8
3	80	100	84.0
4	100	120	101.0
5	120	140	113.0

Figure 2 compares the EUV-FUV reflectance of the ta-C film grown with a bias voltage of 50 V (average ion energy of ~70 eV) with other forms of high-reflectance, solid-state C material; other low-reflectance C-based materials, such as evaporation-deposited films, glassy carbon, and a-C:H films, are not plotted for clarity. ta-C film reflectance approaches that of both bulk and CVD amorphous diamond in the peak-side ranges compared to IBD C films; still, ta-C films do not reach the diamond high peak reflectance at 99 nm. For practical applications of high-EUV reflectance, ta-C-film coated mirrors have the remarkable feature that they are coated on room-temperature substrates, whereas CVD diamond films require a very hot substrate.

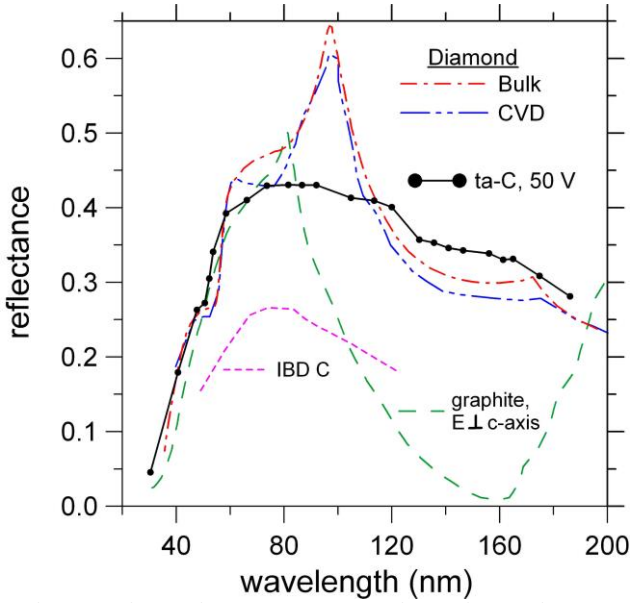

Fig. 2. The EUV-FUV reflectance of a ta-C film compared to other forms of high-reflectance, solid-state C material: bulk diamond [22], CVD amorphous diamond (typical thickness: 15 μm) [24], graphite (E⊥c-axis) [38], IBD C (24-nm thick) [29].

Comparing ta-C films with C films deposited onto non-heated substrates, the former have a significantly higher reflectance than IBD C films. The EUV reflectance of sample 1, grown with 0-V bias voltage, even though lower than that of samples grown with a larger bias voltage, it is slightly larger than the value reported for IBD C films [29]. The reason may be that the average ion energy of sample 1, ~20 eV, even though insufficient to produce C films with highest sp^3 bonding, it is somewhat larger than the average atom energy in an ion-beam sputtering system such as in [29], which may reach only few eV; again, the smaller thickness of the IBD-C sample (24 nm thick) cannot explain a reflectance difference larger than 0.6% (relative) above 55 nm, whereas present sample 1 exceeds IBD C film reflectance an average of 16%. The large reflectance of the ta-C film compared to IBD C is attributed to the high sp^3 bonding content in ta-C films; in this way, diamond represents the limit of 100% sp^3 bonding. The proportion of sp^3 bonding content has been correlated with the energy of the ions in ta-C films [37], and for the present films grown with non-zero bias, the proportion of sp^3 bonding is expected to be in the ~80-85% [34].

The reflectance of graphite for the electric field perpendicular to the c-axis [38] is also plotted in Fig. 2, even though graphite represents the limit of 100% sp^2 bonding content; the reason to plot it here is that its reflectance is large below ~100 nm (conversely, graphite reflectance for the electric field parallel to the c-axis is much smaller [38]).

Figure 3 compares the EUV-FUV reflectance of the ta-C film grown with 50-V bias voltage to that of other thin-film materials with relatively high-reflectance below 120 nm. The

reflectance of IBD-SiC and IBD-B_4C are known to decrease mostly in the first weeks after exposure to atmosphere. Since the present ta-C films were measured after an exposure to the atmosphere of 8 to 9 months, the comparison in Fig. 3 is performed with aged samples of IBD-SiC (80-nm thick) [39] and IBD-B_4C (30-nm thick) [40]. The reflectance of a 58-nm thick Ir film [41] and of a ~70-nm thick Os film [42] are also displayed since these materials have a relatively high reflectance in the ~45-70 nm. Hence, Fig. 3 plots the reflectance of relatively thick films of SiC, B_4C, Ir, and Os. A slightly larger reflectance than the plotted one, mostly for Os, can be obtained for semi-transparent films, and the reflectance increase is due to interferential effects with the substrate. The reflectance of thick films of these materials was selected here because the present ta-C films can be considered also opaque in the high reflectance range, as discussed above, since the attenuation length is much smaller than film thicknesses, and a reflectance increase might be expected with semi-transparent ta-C films as well. Figure 3 shows that the reflectance of ta-C film is larger than that of all other thin-film materials below 130 nm. This result reveals the potential of ta-C films for high-reflectance EUV mirrors.

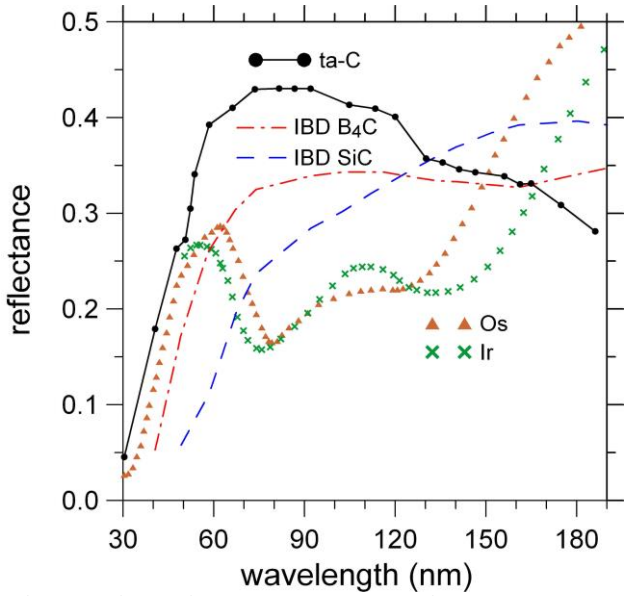

Fig. 3. The EUV-FUV reflectance of a ta-C film compared to other thin-film materials with relatively high reflectance below 120 nm: aged IBD SiC [39], aged IBD B_4C [40], and evaporation-deposited Ir [41] and Os [42].

The roughness of ta-C films deposited with highest sp^3 proportion has been reported to be very small, mostly in the ~0.1 to 0.4 nm range [43,44,45], with smaller roughness for thinner films [31]. These small values are advantageous for the use of ta-C films as EUV mirrors, since surface roughness affects EUV reflectance and scattering more than it does at longer wavelengths.

One drawback of ta-C films is that they grow with a large compressive stress of ~10 GPa, which correlates with the high sp^3 bonding content [46,47]. The high stress limits the maximum film thickness to ~100–200 nm due to adhesion failure [48]; fortunately, a 10-nm thick ta-C film may be thick enough for highest EUV reflectance, although the innermost regions of the thinner films may not grow with as high an sp^3-bonding content as thicker ta-C films do [49]. Friedmann et al. [48] succeeded in releasing the stress of ta-C films by thermal annealing at 600 °C, without destroying the diamond-like properties of the films. Unfortunately, relaxing film stress by annealing at high temperature would limit the benefit of a coating that did not need a hot substrate upon deposition. Other methods to relax stress have been demonstrated. It has been shown that residual stress in ta-C films can be eliminated by

UV excimer laser annealing [50,51] without reducing the fraction of sp^3 bonds; with UV excimer laser annealing, only a localized surface layer of a few hundred nanometers in depth is heated, so that the substrate is not heated in the process. A reduction of ta-C film stress down to ~2 GPa was also obtained by incorporating a fraction of boron in the films without decreasing the high sp^3 bonding content [52]. Hence it seems that one of the main drawbacks of ta-C films for EUV coatings can be handled.

Another difficulty of ta-C films might be the deposition of uniform films on large mirror substrates, from a few centimetres up to meters. In the present system, the deposition area was only 50 mm^2. But the filtered arc source could be made larger for larger size coatings; besides, more than one arc source could be used in parallel. The use of beam scanning, laser-arc process, and sample rotation would also improve homogeneity and scalability. Our estimate is that, at least in one direction, samples as long as 100 cm could be deposited in principle with FCVAD. Alternative deposition processes, such as Pulsed Laser Deposition, are also scalable and produce high sp^3-content ta-C films on larger surfaces [53].

B. Optical constants of ta-C films

The optical constants of ta-C films in the FUV-EUV were calculated with the Kramers-Krönig (KK) analysis using reflectance data. The modulus $R^{1/2}$ and phase φ of complex reflectance $r=R^{1/2}\exp(i\varphi)$ are linked with the following dispersion relation:

$$\varphi(E) = -\frac{E}{\pi} P \int_0^{\infty} \frac{\ln[R(E')]}{E'^2 - E^2} dE' \qquad (1)$$

where P stands for the Cauchy principal value. Equation (1) provides the reflectance phase φ by integration of the reflectance modulus, from which it is straightforward to calculate *n* and *k* using the well-known Fresnel reflectance formula at normal incidence. The present EUV-FUV reflectance measurements were performed at 5° from the normal and no significant difference from normal-incidence reflectance is expected. The integral is presented in terms of photon energy E instead of wavelength to show it in the most common way. To perform the integration of Eq. (1) we need a full set of reflectance data in the whole spectrum. We extended the present reflectance measurements to cover the spectrum for an opaque ta-C film. At shorter wavelengths (larger photon energies) than present measurements, we used the semi-empirical data of Henke et al. [54], which assumes that the atoms interact with radiation independently of the other atoms. The Henke data were downloaded from the Web site of The Center for X-Ray Optics (CXRO) at Lawrence Berkeley National Laboratory [55]. A density of 3.25 g/cm^3 was assumed [56]. Both k and $n=1-\delta$ data were downloaded to calculate reflectance. Henke data were used in the energy range of 30 to 30,000 eV. For energies larger than 3×10^4 eV, we extrapolated Henke data by keeping constant the slope of the log-log plot of *k*(E). Figure 1 also displays reflectance calculated with Henke data for an opaque film.

In the 190-950-nm range, reflectance was calculated using the optical constants obtained from ellipsometry measurements. Ellipsometry measurements in the 190-950-nm spectral range were performed on the sample grown with a bias voltage of 50 V. Figure 4 displays the measured ellipsometry parameters:

$$\frac{\mathbf{r_p}}{\mathbf{r_s}} = \mathbf{tan}(\Psi) e^{i\Delta} \qquad (2)$$

Measurements were performed at 68°. To fit the ellipsometry measurements in order to calculate *n* and *k*, we used various Lorentz oscillators. A good fit to the ellipsometry measurements was obtained with a set of three Lorentz oscillators:

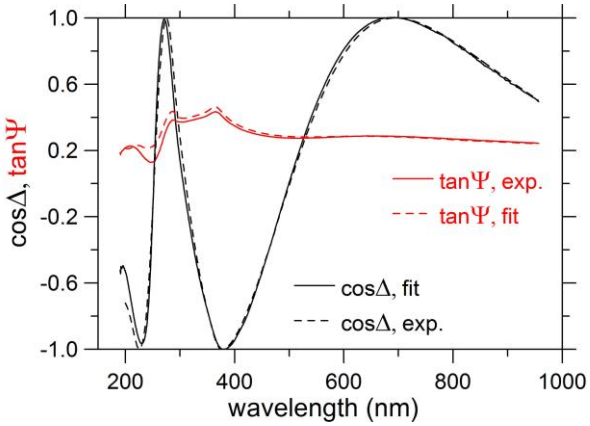

Fig. 4. Ellipsometry parameters tan Ψ and cos Δ, both experimental and fitted with the obtained *n*, *k* data, as a function of wavelength measured for the ta-C film deposited with 50-V bias voltage.

$$\varepsilon = (n+ik)^2 = \sum_{j=1}^{3} \frac{-A_j E_{0j}}{E^2 - {E_{0j}}^2 + iC_j E} \tag{3}$$

where ε is the dielectric constant, the square of the complex refractive index *n*+i*k*. The oscillator parameters of the fitting are given in Table 2.

Table 2. Parameters of the three Lorentz oscillators obtained in the fitting to ellipsometry measurements.

Parameters	Oscillator 1	Oscillator 2	Oscillator 3
A (eV)	55.15	1.63	4.56
E_0 (eV)	11.03	4.58	6.14
C (eV)	0.0087	1.74	1.82

The three Lorentz oscillators of the fitting were used to obtain *n* and *k* in the ellipsometry range and they were also used for the extrapolation to longer wavelengths. These *n* and *k* data were used to calculate reflectance in this range for an opaque film, which completed the reflectance set to perform the KK analysis using Eq. (1). The match between the long-wavelength reflectance measurements and the reflectance calculated with ellipsometry data was improved with a smooth adaptation. KK analysis resulted in a self-consistent set of *n* and *k* data.

Figure 5 displays the obtained *n* and *k* data, along with Henke data. Figure 1 also displays the reflectance calculated with the obtained *n*, *k* data; there is a good coincidence in the EUV-FUV reflectance between experimental measurements and calculations. Reflectance deviations are important only above ~170 nm; in this long FUV range *k* is smaller so that reflectance becomes more dependent on thickness. In Fig. 1, measured reflectance is somewhat higher than reflectance calculated with Henke data; the difference might be attributed to that Henke's independent-atom approach may not be fully accurate in this long-wavelength edge. Henke's approach is typically accepted below ~41 nm and away from absorption edges. The coincidence range is limited here to this long Henke edge, where ta-C absorption is still relatively high, in the tail of the high-reflectance peak at ~90 nm. Figure 4 compares the ellipsometry measurements with the ellipsometry parameters calculated with the obtained *n* and *k* data, which results in a good match.

The consistency of the calculated optical constants was evaluated with two sum-rules. The f-sum rule calculates the effective number of electrons per atom $n_{eff}(E)$ contributing to *k* up to a given photon energy:

$$n_{eff}(E) = \frac{4\varepsilon_0 m}{\pi N e^2 \hbar^2} \int_0^E E' k(E') dE' \tag{4}$$

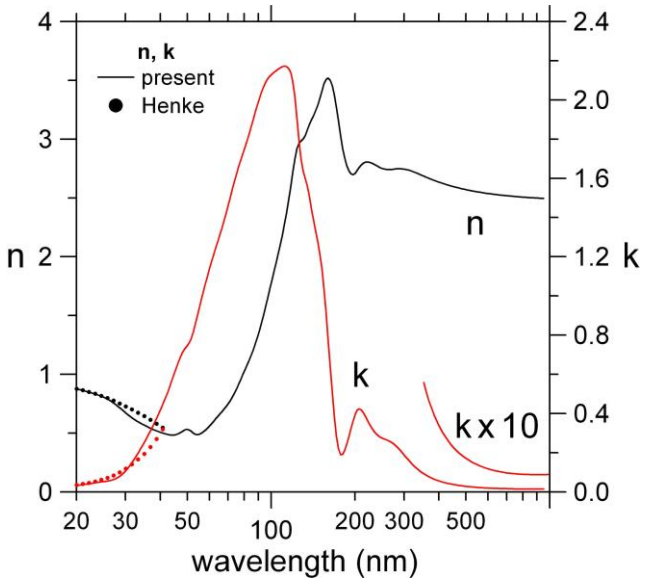

Fig. 5. The optical constants *n* and *k* of ta-C versus wavelength in log scale. The semi-empirical data of Henke et al. [54] are also shown.

where N is the atom density (a mass density value of 3.25 g/cm^3 was used), e and m are the electron charge and mass, respectively, ε_0 is the permittivity of vacuum, and $\hbar$ is the reduced Planck's constant. The f-sum rule indicates that the high-energy limit of the $n_{eff}(E)$ must be 6, the atomic number of C. When the relativistic correction on scattering factors is taken into account, $n_{eff}(E)$ high-energy limit is slightly modified: the theoretical effective number of electrons is reduced to 5.994 [57]. The integral of Eq. (4) with the present *k* data results in 5.95, a mere 0.8% lower than the theoretical value.

The inertial sum-rule rule:

$$\int_0^\infty [n(E) - 1] dE = 0, \tag{5}$$

expresses that the average refractive index over the spectrum is unity. The following normalization parameter was used to evaluate the fulfillment of Eq. (5) [58]:

$$\zeta = \frac{\int_0^\infty [n(E) - 1] dE}{\int_0^\infty |n(E) - 1| dE} \tag{6}$$

According to Shiles et al. [59], a good value of ζ must stand within ±0.005. A value of ζ=-2 $\times 10^{-4}$ was obtained with the present *n* data set. Therefore, both the *f*- and the inertial-sum rules are satisfactorily met, which suggests a good accuracy of the present optical constants of ta-C.

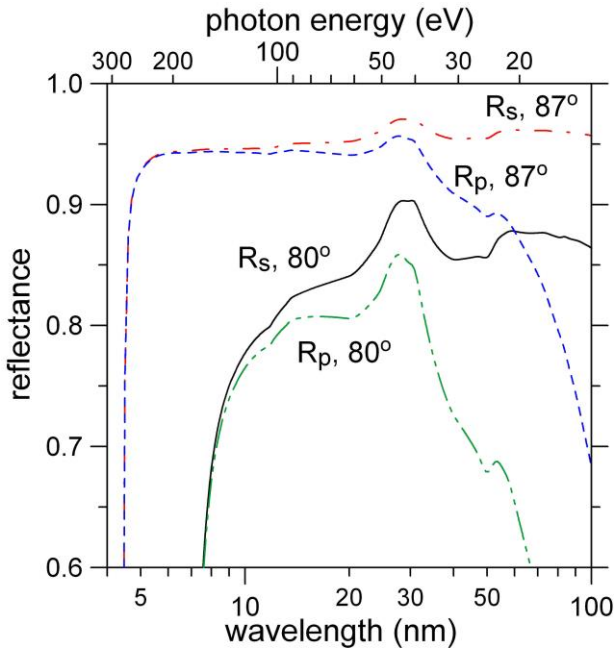

Fig. 6. Calculated ta-C EUV reflectance at two grazing incidence angles measured from the normal versus wavelength in log scale.

The stability of carbon films, along with their relatively high reflectance at grazing incidence, make C films a good choice for FEL mirrors. Several EUV FELs presently in operation involve mirrors based on sputter-deposited amorphous carbon films [60]. In this application, mirrors operate at grazing incidence to reduce radiation density on the coating, which results in a high reflectance in a wide spectral range of up to a photon energy of ~200 eV. The mechanical hardness, chemical inertness, and thermal stability of ta-C films make them a promising candidate for FEL mirrors. The optical constants obtained for ta-C films allow us to calculate their reflectance in order to evaluate their potential for applications such as mirrors for a FEL. Figure 6 displays the calculated reflectance of ta-C films at two grazing incidence angles, 80° and 87°, for radiation polarized both in the incidence plane (p) and perpendicular to it (s); the above *n*, *k* data were used in the calculation; below ~20 nm, the difference between the present data set and Henke data was negligible. A high reflectance is calculated in a broad range, which extends well above 200 eV for 87°-incidence due to the relatively high ta-C density, until a steep reflectance decay is obtained close to the C K edge.

The reflectance and (*n*, *k*) data are available on request at the following e-mail address: larruquert@io.cfmac.csic.es.

Conclusions

The EUV reflectance of ta-C films deposited with average ion-energy varying in the ~70-140-eV range has been proved to be significantly larger than for C films grown with lower atom energies, such as sputtering- or evaporation-deposited C films. No significant reflectance difference was observed among films within the above ion energy range. The reflectance of C films deposited with a lower average ion-energy of ~20 eV was smaller than in the above larger energy range. The reflectance of ta-C films approaches the reflectance of diamond (compared to sputtered-deposited C), although with a lower peak, but with the advantage that ta-C films are deposited on room-temperature substrates. The EUV reflectance of ta-C films is higher than for all other aged coatings of usual materials in the whole EUV-FUV range below 130 nm. A drawback of ta-C films may be the presence of a larger intrinsic compressive stress

particularly for thicker layers but it is however expected to be surmountable according to several reported methods for stress relaxation.

Self-consistent optical constants of ta-C films in the EUV to the near infrared have been calculated by KK analysis using near-normal reflectance measurements in the 30-188-nm range and ellipsometry measurements in the 190-950 nm range, along with extrapolations. A good consistency of the data was evaluated with the application of two sum rules. The obtained optical constants resulted in a high grazing-incidence calculated reflectance in the EUV to soft-X-rays up to photon energies well above 200 eV. The relatively high reflectance, along with the material inertness and hardness, make ta-C films a promising material for applications in harsh environments, such as FEL mirrors.

Acknowledgments

This work was partially supported by the National Programme for Space Research, Subdirección General de Proyectos de Investigación, Ministerio Economía y Competitividad, Project No. AYA2010-22032. L. Rodríguez-de Marcos is thankful to Consejo Superior de Investigaciones Científicas (CSIC) for funding under the Programa JAE, partially supported by the European Social Fund.